

Electronic Supplementary Information

Coordination Polymers of Fe(III) and Al(III) Ions with TCA Ligand: Distinctive Fluorescence, CO₂ Uptake, Redox-Activity and Oxygen Evolution Reaction

Barun Dhara,^a Subrahmanyam Sappati,^b Santosh Singh,^c Sreekumar Kurungot,^c
Prasenjit Ghosh^{a,b} and Nirmalya Ballav^{*a}

^a Department of Chemistry, IISER Pune, India.

^b Department of Physics, IISER Pune, India.

^c Centre for Energy Science (CES), IISER Pune, India.

^dPhysical & Materials Chemistry Division, CSIR-NCL Pune, India.

Electrochemical Characterization:

All the electrochemical analyses have been performed by using an instrument VMP-3 model Biologic potentiostat. A conventional three electrode setup containing glassy carbon (GC) coated with catalyst, graphite rod and Hg/HgO as a working electrode (W.E), counter electrode (CE) and reference electrodes (RE) respectively, used as an electrochemical cell. An aqueous solution containing 1M KOH was used as electrolyte. The potentials obtained w.r.t Hg/HgO were converted w.r.t. RHE. The GC electrode was polished by 0.3 μm alumina slurry before coating the catalyst on it. The catalyst slurry was prepared by mixing 90% active material, 10% acetylene black and 40 μL 5% Nafion in 1 mL 3:2 (IPA:water) solution followed by bath sonication for 1h. To the polished GC electrode, 10 μL of the prepared slurry was coated and kept under an IR lamp for drying. For the electrocatalytic studies cyclic voltammetry (CV), linear sweep voltammetry (LSV) has been performed.

Gelation Test:

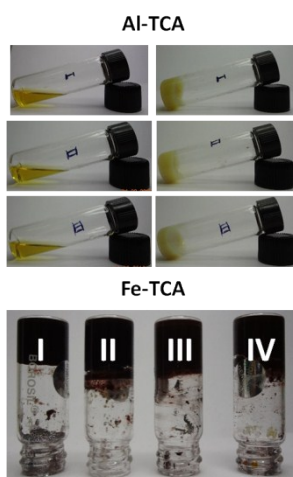


Fig. S1 Gelation test of different batches of TCA ligand with aluminium nitrate (upper) and with ferric nitrate (bottom).

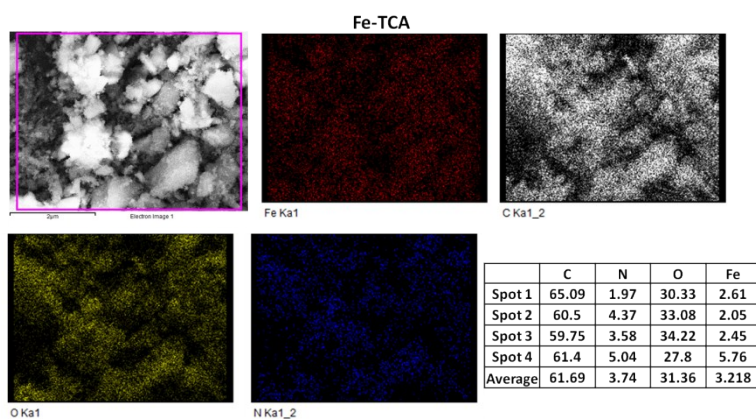


Fig. S2 EDXS analysis and elemental mapping of Fe-TCA xero-gel material.

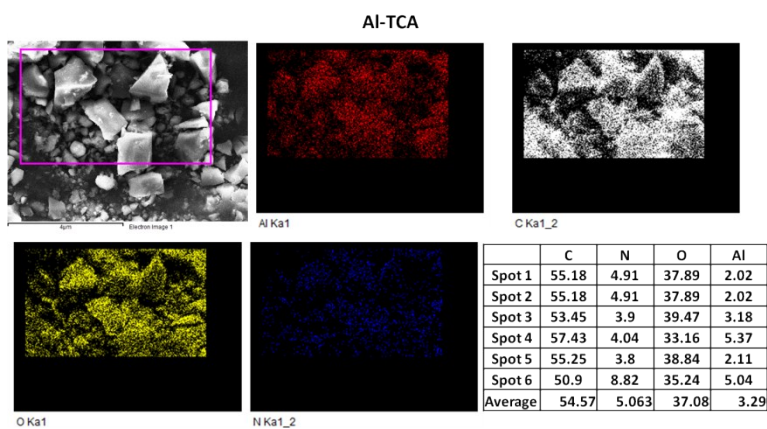


Fig. S3 EDXS analysis and elemental mapping of Al-TCA xero-gel material.

Table S1 Different spin configurations for the Fe-Bz.

Spin Multiplicity	Total energy (Hartree)	Relative energy w.r.t 21et (eV)
Singlet	-4390.53559183	4.91
Triplet	-4390.62974416	2.35
11et	-4390.66276798	1.45
21et	-4390.71592470	0

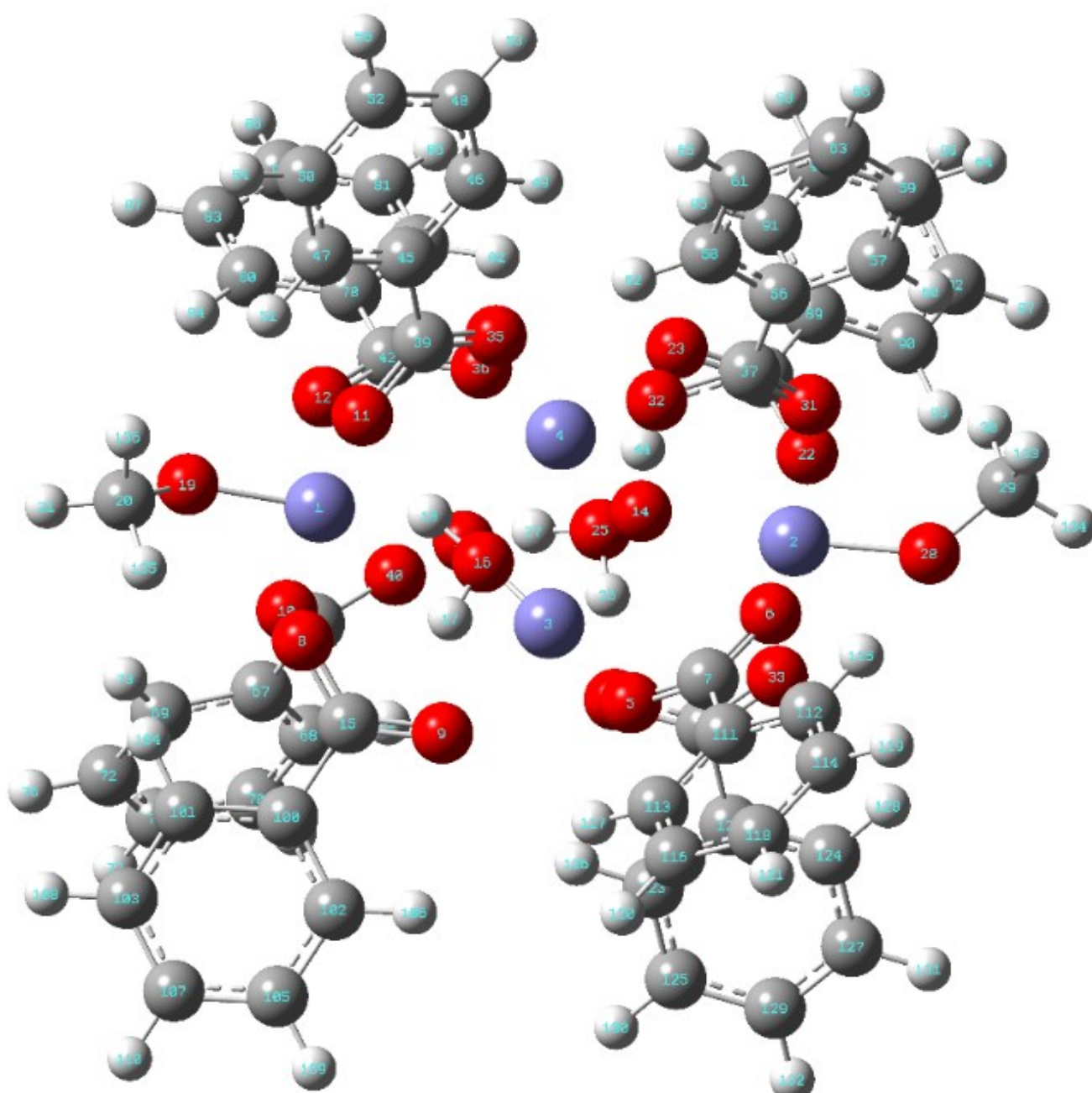


Fig. S4 Ground state structure of Fe-Bz.

Table S2 Fe-Fe and Fe-oxygen bond distances for Fe-Bz

	Distance (Å)		Distance (Å)
Fe1-Fe3	3.57	Fe2-Fe3	3.48
Fe1-Fe4	3.41	Fe3-Fe4	2.90
Fe4-Fe2	3.66	Fe2-O28	1.82
Fe1-O13	2.00	Fe2-O31	2.20
Fe1-O11	2.15	Fe2-O22	2.08
Fe1-O12	2.03	Fe2-O14	2.10
Fe1-O19	1.83	Fe2-O33	2.09
Fe1-O10	2.31	Fe2-O6	2.08
Fe1-O8	2.11	Fe3-O16	2.23
Fe4-O35	2.04	Fe3-O14	1.95
Fe4-O36	2.09	Fe3-O5	2.04
Fe4-O13	2.00	Fe3-O34	2.07
Fe4-O25	2.24	Fe3-O9	2.07
Fe4-O14	1.97	Fe3-O13	1.93
Fe4-O23	2.01		

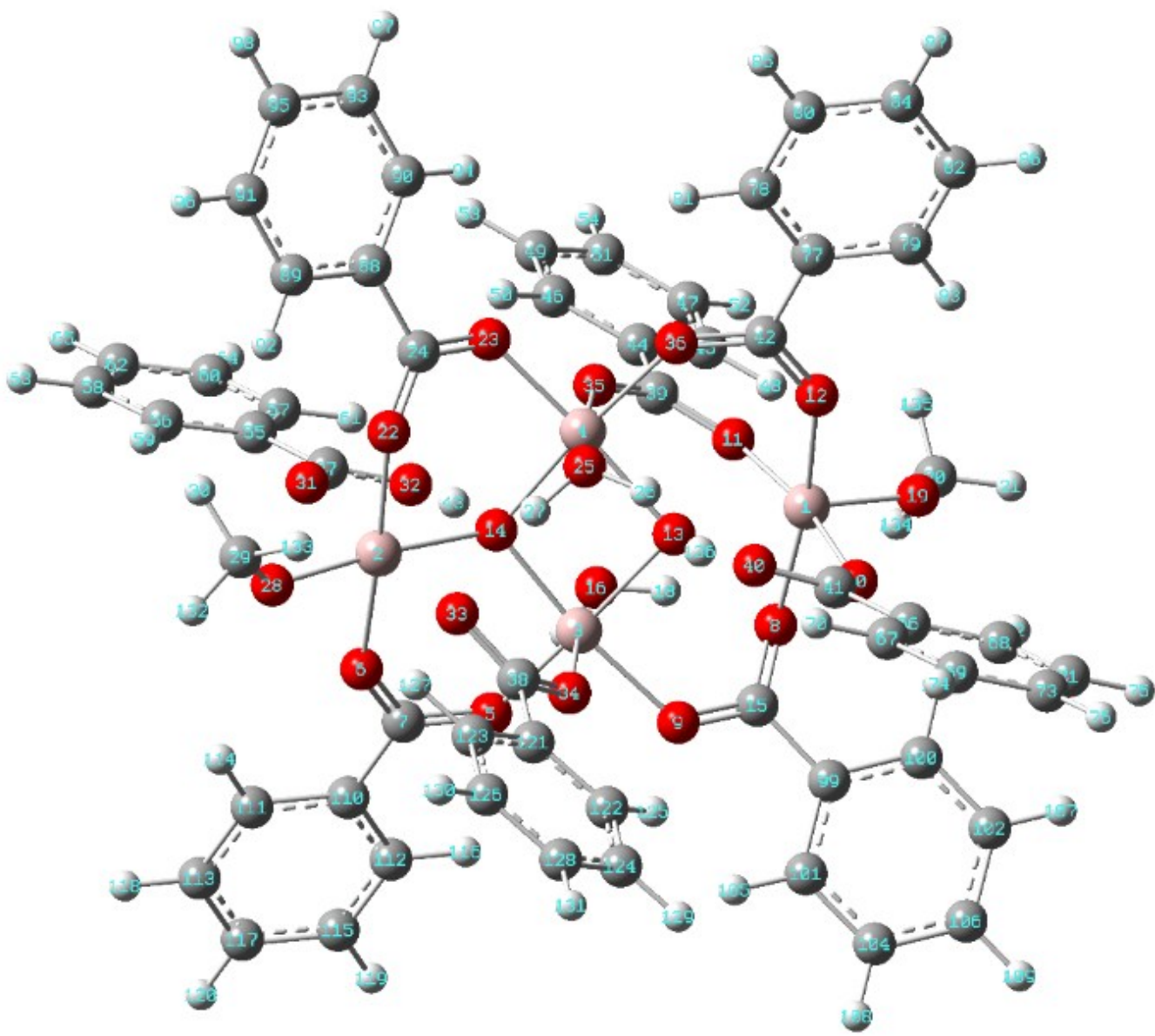


Fig. S5 Ground state structure of Al-Bz.

Table S3 Al-Al and Al-oxygen bond distances for Al-Bz

	Distance (Å)		Distance (Å)
Al1-Al3	3.70	Al2-Al3	3.34
Al1-Al4	3.57	Al3-Al4	2.95
Al4-Al2	3.43	Al2-O28	1.78
Al1-O13	2.13	Al2-O31	2.04
Al1-O11	2.00	Al2-O22	1.97
Al1-O12	1.92	Al2-O14	1.96
Al1-O19	1.78	Al2-O33	2.03
Al1-O10	2.00	Al2-O6	1.97
Al1-O8	2.02	Al3-O16	2.04
Al4-O35	1.91	Al3-O14	1.89
Al4-O36	1.92	Al3-O5	1.91
Al4-O13	1.98	Al3-O34	1.91
Al4-O25	2.05	Al3-O9	1.95
Al4-O14	1.92	Al3-O13	1.98
Al4-O23	1.90		

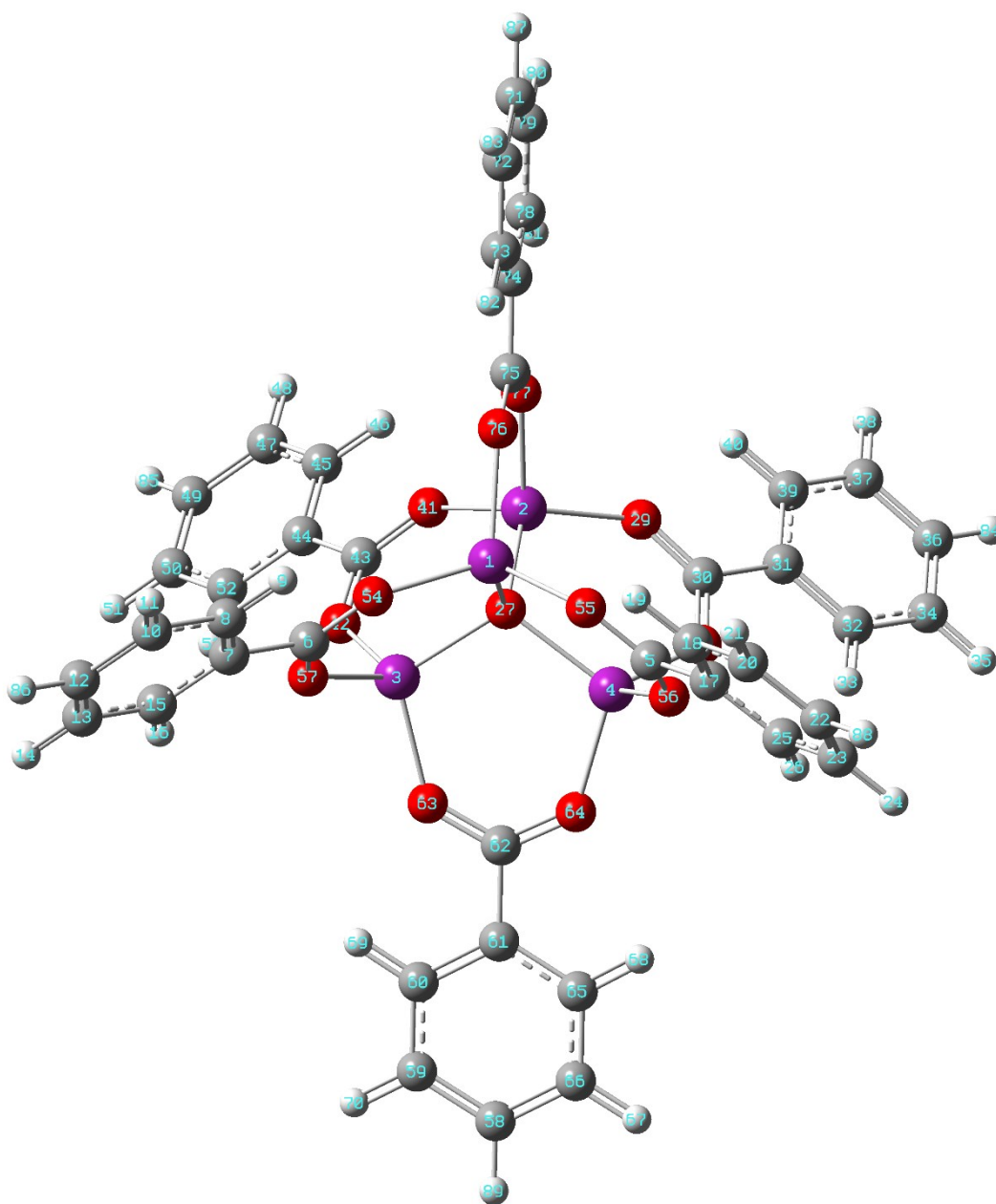


Fig. S6 Ground state structure of Zn-Bz (all the Zn-oxygen bond lengths are equal to 2.00 Å).

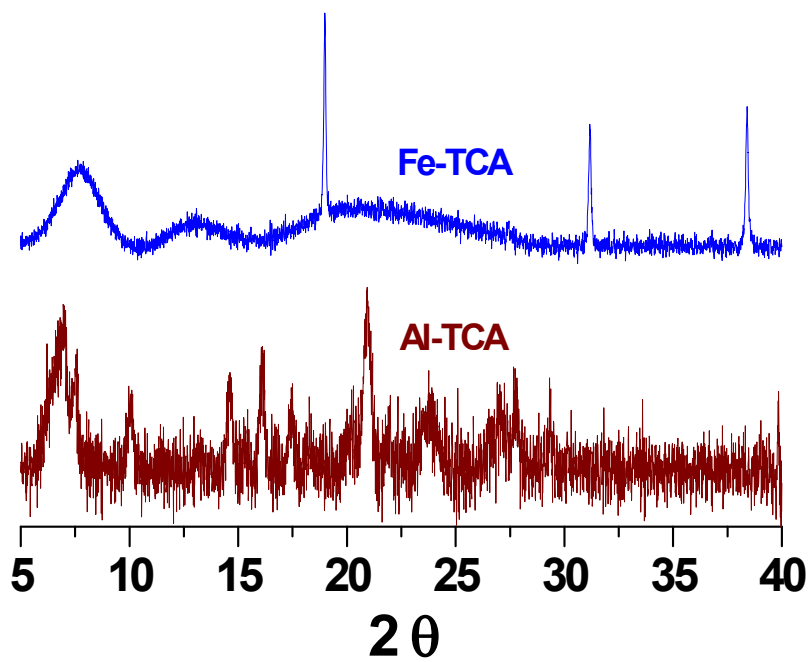


Fig. S7 PXRd patterns of Al-TCA (wine red) and Fe-TCA (blue) xerogels which indicated the semi-crystalline nature.

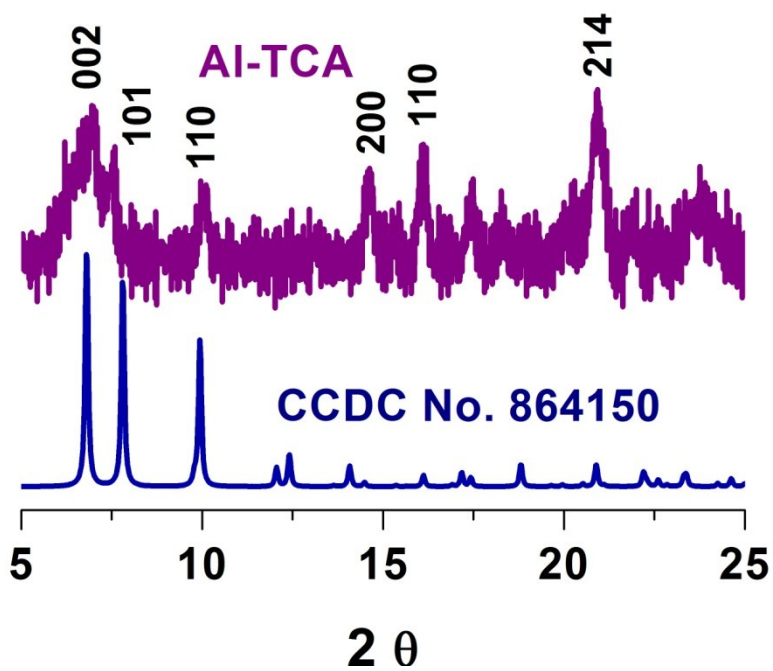


Fig. S8 PXRd patterns of Al-TCA (violet) and Ho-TCA (dark blue; simulated from its crystal structure).

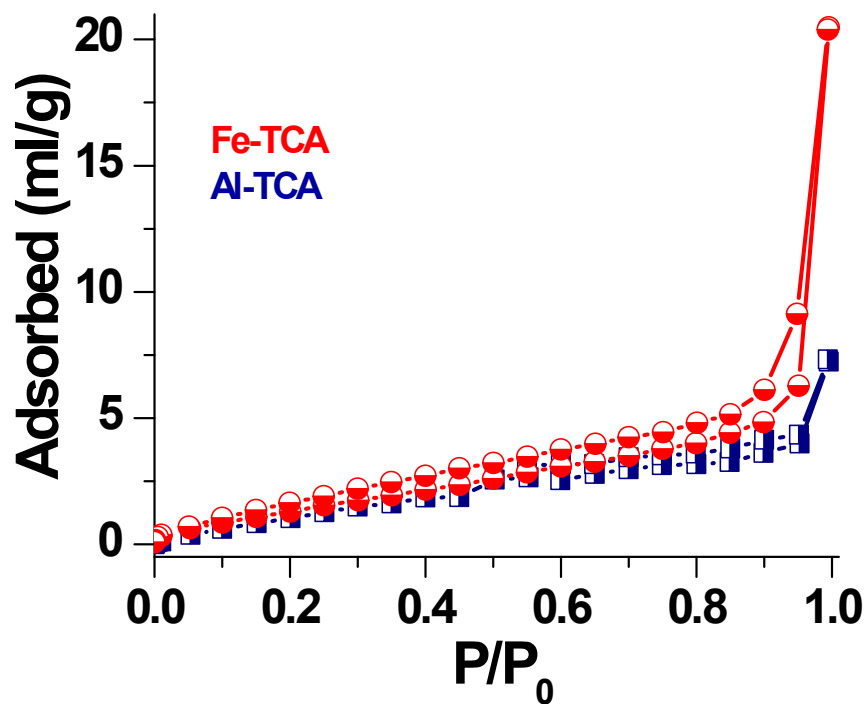


Fig. S9 N_2 gas adsorption study on Fe-TCA (red), and Al-TCA (blue) xerogels at 195K.

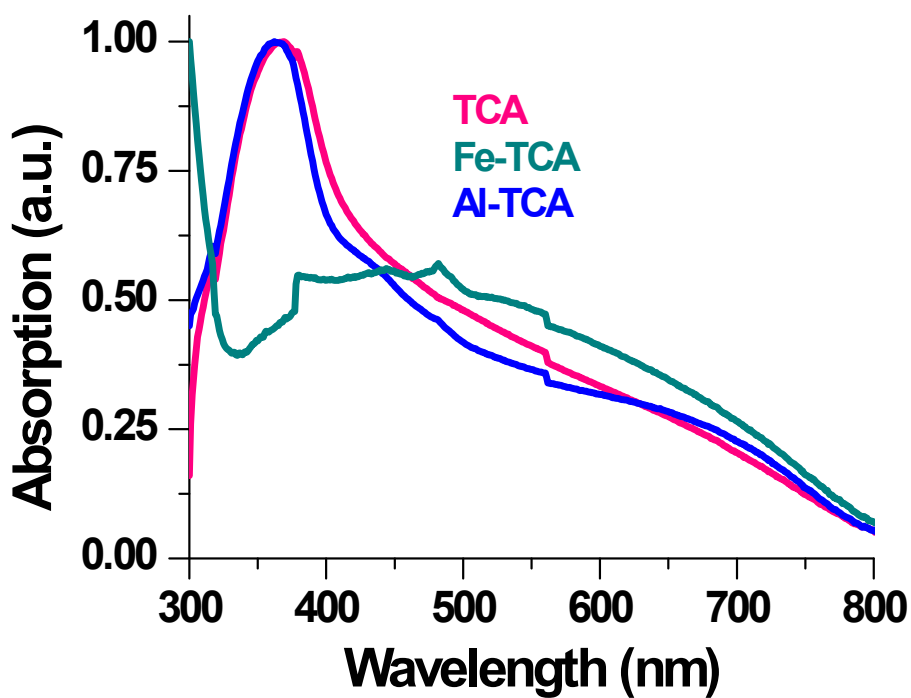


Fig. S10 UV-vis spectra of xerogel materials where absorption band at 365 nm of TCA (pink) and Al-TCA (blue) was vanished in Fe-TCA (green) xerogel.

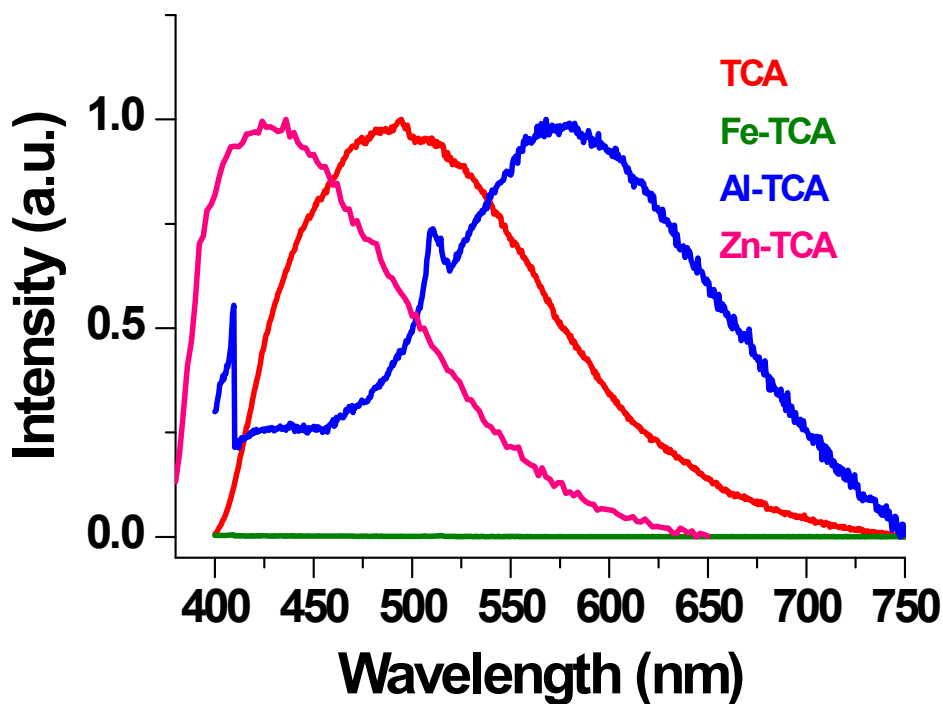


Fig. S11 The solid state fluorescence spectra of TCA (Red), Fe-TCA (green), Al-TCA (blue) and Zn-TCA (pink) compounds with excitation wavelength of 350 nm.

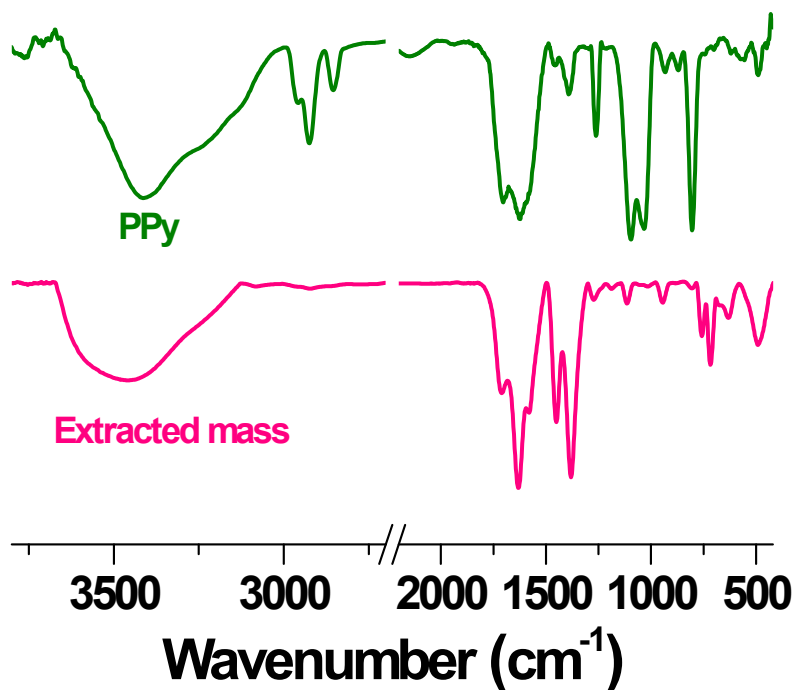


Fig. S12 FTIR spectra of the extracted materials (pink) from Fe-TCA@Py and PPy prepared by using oxidising agent (green). Both FTIR spectra were looked very similar.

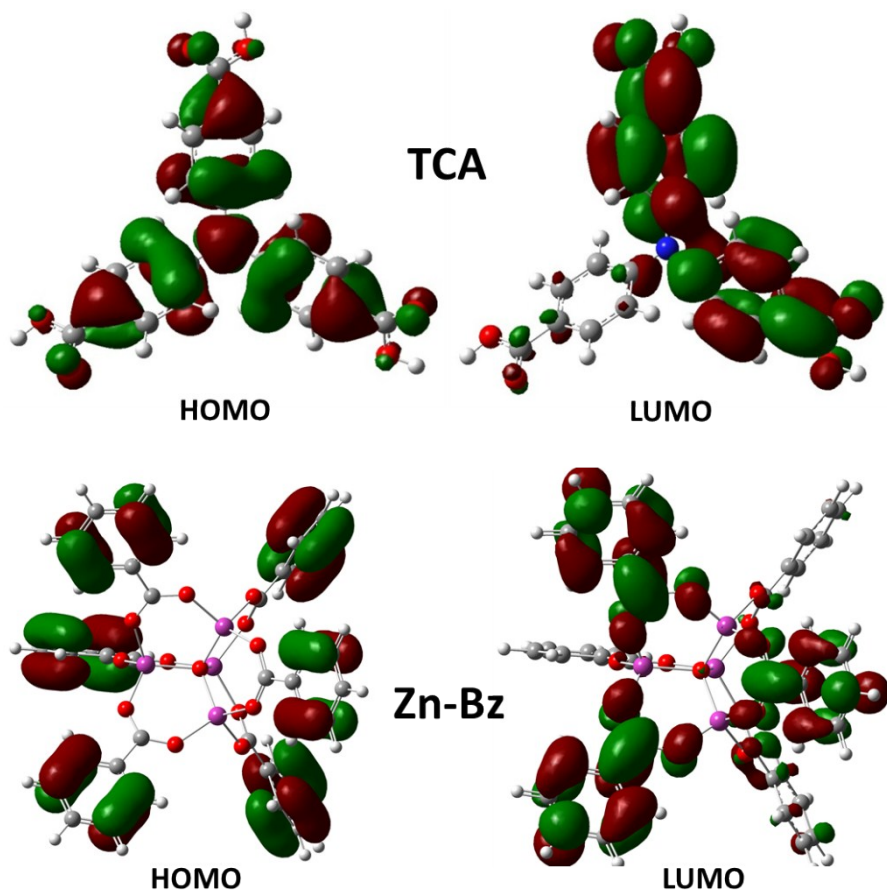


Fig. S13 HOMO and LUMO of TCA (upper) and Zn-Bz (lower).

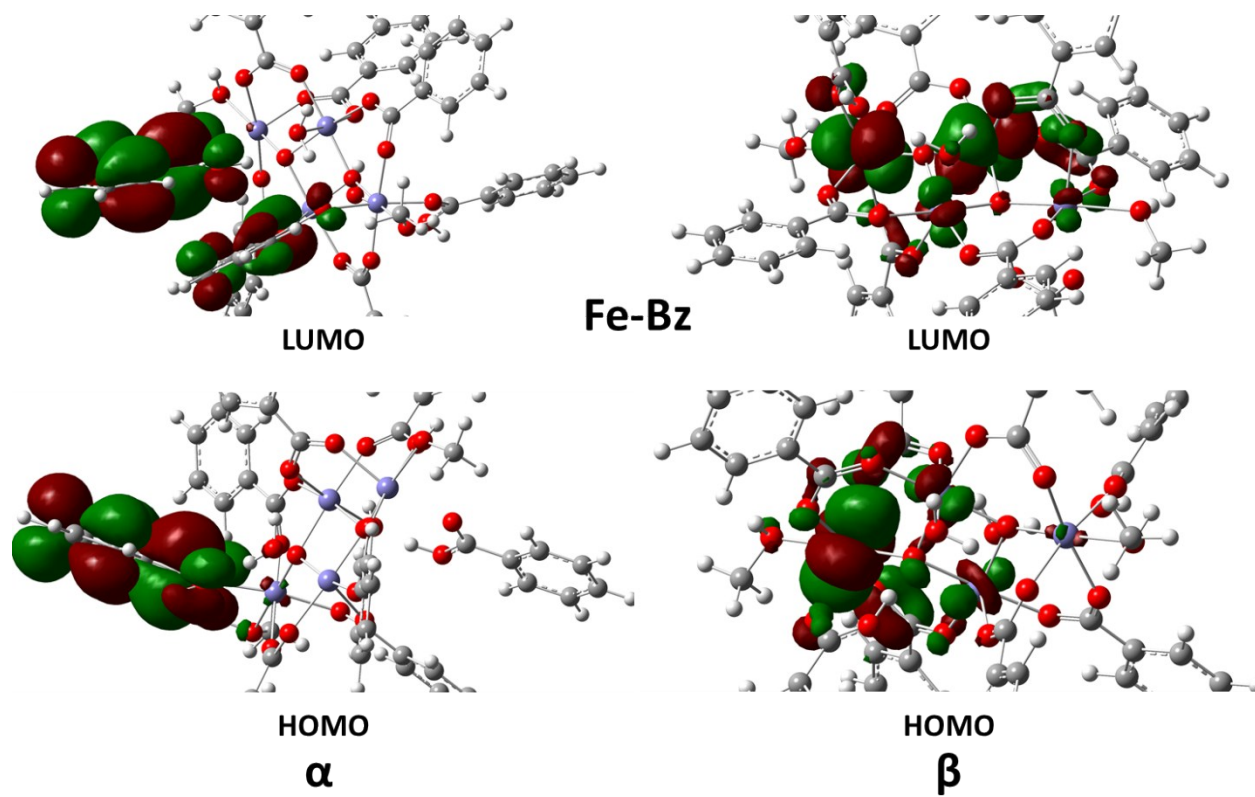


Fig. S14 HOMO and LUMO of alpha (left) and beta Fe-Bz.

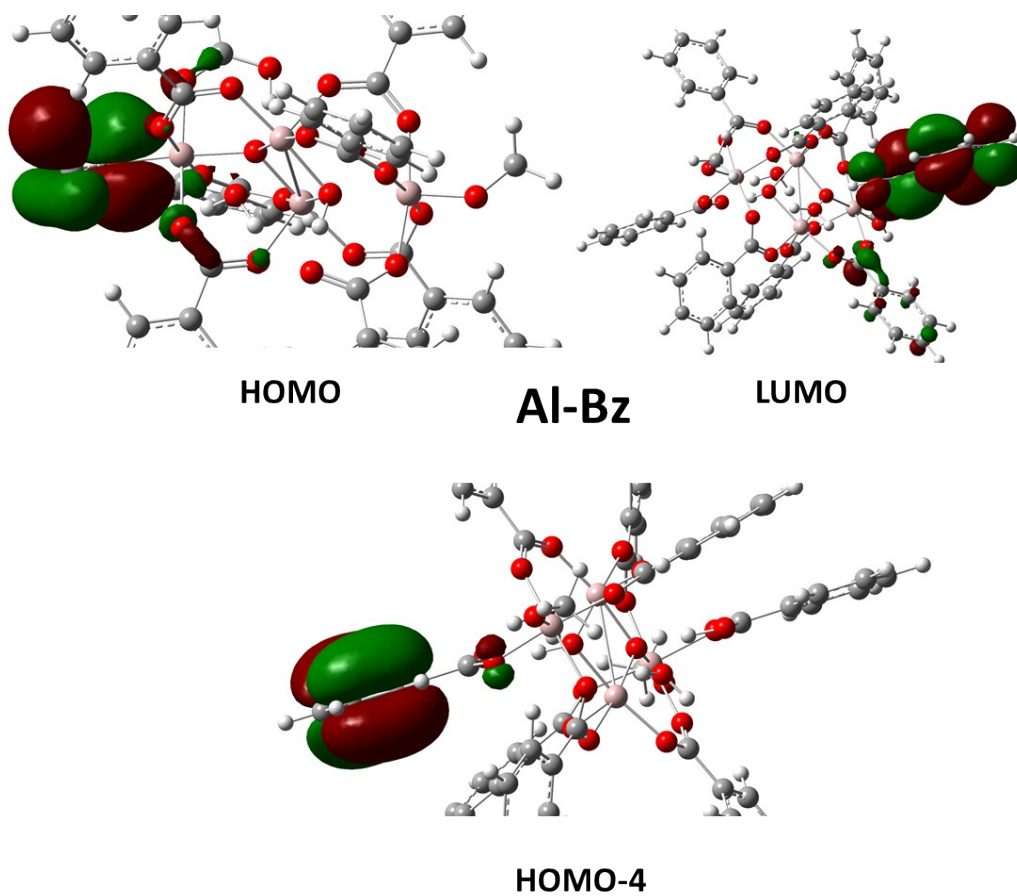


Fig. S15 HOMO (upper left) and LUMO (upper right) and LUMO-4 (lower) of Al-Bz.

Table S3 HOMO and LUMO band gaps of TCA and composite materials of aluminium, iron and zinc with benzoic acid.

System	HOMO (eV)	LUMO (eV)	Diff (eV)
TCA	-5.71	-1.73	3.98
Fe-Bz (α)	-6.01	-2.12	2.87
Fe-Bz (β)	-6.14	-3.14	
Zn-Bz	-6.88	-1.24	5.64
Al-Bz	-5.35	-1.62	3.73
Benzoic acid	-7.08	-1.31	5.77

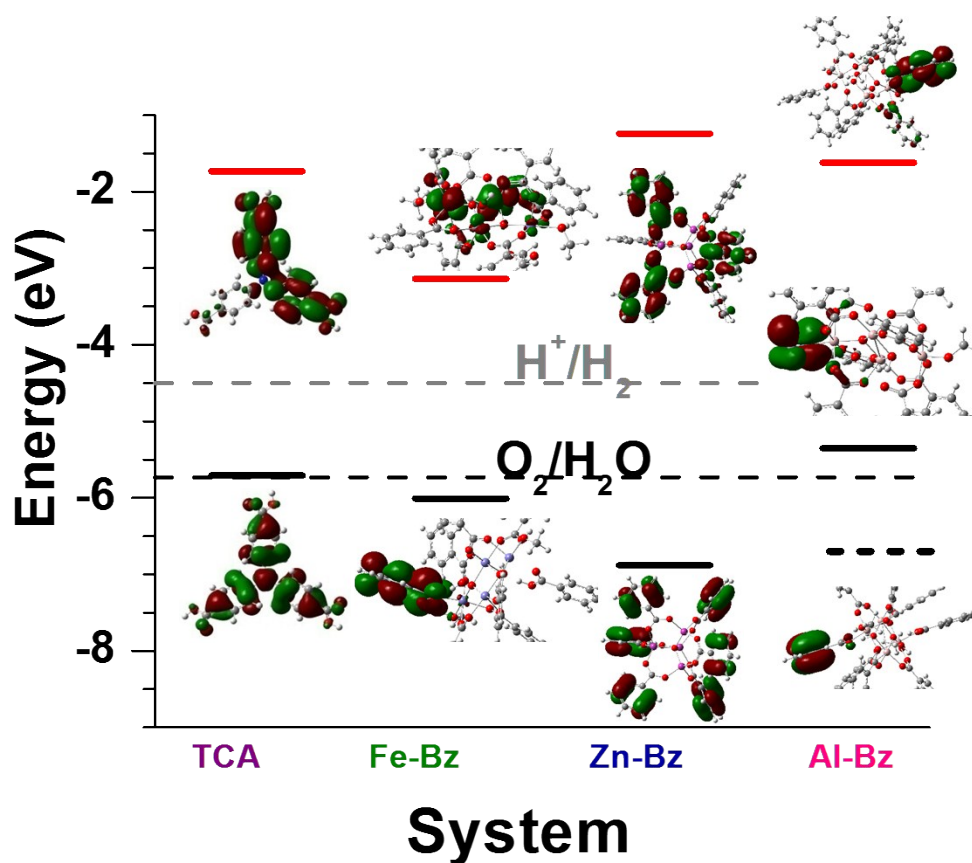


Fig. S16 The energy diagram of TCA and composite materials of aluminium, iron and zinc with benzoic acid. Their corresponding HOMO (black) and LUMO (red) are placed. The dashed black line corresponds to HOMO-4 Eigen state of the Al-complex which is coming from ligand. The dashed grey and blue lines mark the OP and RP of water splitting.